COMPARATIVE ANALYSIS OF ADVANCED CONTROL STRATEGIES FOR MODERN AIRCRAFT DYNAMICS

S. Singh*, W. Meyer-Brügel* and F. J. Silvestre*
* Flight Mechanics, Flight Control and Aerolelasticity, Marchstr. 12, 10587 Berlin, Germany

Abstract

Modern aircraft design, driven by advancements in materials and aerodynamic optimisations as well as new applications and unconventional configurations, especially in the UAV sector, but also for medium to large transport aircraft, exhibits complex dynamic behaviour that challenges conventional flight control systems. In consequence, several modern control approaches have emerged, which all have in common to strive for a reduced plant dependency by utilising acceleration or state derivative measurements and thereby extending the control scope to the actuator dynamics. This paper presents a comparative analysis of four advanced control approaches using the well-established Non-linear Dynamic Inversion (NDI) as a reference: Local Acceleration Control (LAC), Incremental Non-linear Dynamic Inversion (INDI), Extended Incremental Non-linear Dynamic Inversion (E-INDI) and Actuator Non-linear Dynamic Inversion (ANDI). We draw attention to the strong analogies between these approaches, which are still inadequately recognised in the field. In the first part of the paper each control law is formulated using a consistent, unique nomenclature and applied to a simple flight dynamic system of an aircraft represented as a point mass to facilitate a comparison of their structures. It is shown that some of these approaches converge to the same control law under ideal nominal conditions. In the second part of the paper, the approaches are evaluated by simulation, extending to various non-ideal conditions, including sensor dynamics, rate dynamics, and model uncertainties. These real-world effects compromise the cancellation of feedback loops inherent to the incremental control concepts, causing results to differ in practice despite all analogies. The advantages and problems of the approaches are presented, with particular emphasis on LAC, which shares the benefits of the INDI-based approaches in terms of robustness, disturbance rejection and compensation of non-linearities, but takes additional advantage from a direct actuator level implementation, avoiding asynchronous, counteracting feedback and enabling lower lag times as well as straightforward gain adjustment.

NOMENCLATURE

Symbols

A	State Matrix
B	Input Matrix
C	Output Matrix
f	Frequency
h	Altitude
J	Moment of Inertia
K	Static Controller Gain
ν	Pseudo Command
ω_0	Undamped Natural Frequency
s	Laplace Variable
u	Control Deflection
Z	Linear Dependencies
ζ	Damping Coefficient

Indices

act	Actuator
c	Command
c	Cut-off
des	Desired
mod	Modified

Abbreviations

ANDI	Actuator Non-linear Dynamic Inversion
E-INDI	Extended Incremental Non-linear Dynamic Inversion
EoM	Equation of Motion
INDI	Incremental Non-linear Dynamic Inversion
LAC	Local Accerlation Control
NDI	Non-linear Dynamic Inversion
SSE	Steady-State Error

1. INTRODUCTION

In classical flight control architectures, flight control laws are developed independently of the actuator internal control law. This separation is justified by the assumption that actuator dynamics are sufficiently fast for many conventional flight control applications. However, advancements in aircraft design, driven by new materials, aerodynamic optimisations and lightweight structures, have led to increased structural flexibility, particularly in high-aspect-ratio configurations. These changes introduce dynamic behaviours that require active stabilisation in a broader frequency range. [1,2]

©2026 doi: 10.25967/650399

To address these challenges, recent research has focused on flight control laws that consider actuator dynamics in the flight control design phase. One such method is the Local Acceleration Control (LAC) approach proposed by Meyer-Brügel and Silvestre [3]. The LAC approach directly modifies the actuator control loop by removing the conventional actuator position feedback loop and replacing the commanded deflection angle with the local acceleration generated at the control surface, allowing for greater disturbance rejection and superior robustness with respect to aerodynamic parameter uncertainties [3].

Acceleration measurements also play an important role in various non-linear control approaches. The Non-linear Dynamic Inversion (NDI) approach inverts the non-linearities of the system, resulting in a linear relation between the commanded auxiliary control input and the system output [4]. However, this method is dependent on an accurate mathematical system model [5]. The Incremental Non-linear Dynamic Inversion (INDI) approach overcomes this limitation by computing an incremental control input based on actual measurements of the state derivatives (e.g. accelerations) rather than computing them model based. This reduces dependence on the full system model to the influence of the input effectivity, thus increasing robustness dramatically [5, 6]. However, a key disadvantage is that the actuator dynamics are not explicitly taken into account.

Building on the INDI approach, Raab et al. propose an Extended Incremental Non-linear Dynamic Inversion (E-INDI) approach that incorporates actuator dynamics directly into the inversion process [7]. This allows for an artificial modification of actuator dynamics during controller design. However, the E-INDI approach does not account for state-dependent terms during the inversion process. Steffensen et al. propose a sensor-based Actuator Non-linear Dynamic Inversion (ANDI) approach, which integrates actuator dynamics and state-dependent terms into the incremental control law [8]. All these incremental control approaches have in common to introduce a positive feedback of the actuator position (as they command increments relative to that position). Thereby, they do essentially invert the actuator (position-) dynamics, as the positive feedback cancels the negative position feedback inherent to almost any servo control algorithm [5]. In consequence, although originating from totally different perspectives, the LAC approach (intentionally modifying the actuator control) on the one hand and the INDI related control approaches (inverting the actuator dynamics imposed by the controller) on the other hand result in very similar control laws and do partially share the same benefits. However, due to the never achievable perfect cancellation of the two contradicting feedback loops which are based on independent measurements and realised in separate hardware units, the practical results are expected to differ.

This paper aims to compare these five control approaches: LAC, NDI, INDI, E-INDI and ANDI and to investigate the influence of typical effects leading to non-ideal cancellation of the loops and their practical impact on control performance. In Section 2, the flight dynamics and actuator models are introduced. Section 3 formulates each control approach using a consistent, unique nomenclature and expresses all control laws in terms of a commanded actuator speed, enabling a clearer comparison of their structures. Section 4.1 evaluates nominal performances of the approaches, including the ability of the LAC, E-INDI and ANDI approaches to modify the actuator dynamics. Section 4.2 investigates robustness with respect to sensor models, rate dynamics and model uncertainties. Finally, Section 5 concludes the paper.

2. MODELLING

2.1. Flight Dynamics Model

To point out the underlying principles and the analogies between the different control approaches, in best clarity, a very basic example, as in [3], will be employed. This example considers a point-mass aircraft model with only the plunge degree of freedom. The simplified equation of motion (EoM) is expressed as

$$\ddot{h} = -Z_u u - Z_\alpha \dot{h}, \tag{1}$$

where h is the altitude, u is the elevator deflection, Z_α and Z_u express the lift force linear dependencies associated with a reference flight condition. This EoM can also be written as a state-space model:

$$\begin{aligned} \dot{x} &= Ax + Bu, \\ y &= Cx, \end{aligned} \tag{2}$$

where

$$A = \begin{bmatrix} 0 & 1 \\ 0 & -Z_\alpha \end{bmatrix},\ B = \begin{bmatrix} 0 \\ -Z_u \end{bmatrix},\ C = \begin{bmatrix} 1 & 0 \end{bmatrix},\ x = \begin{bmatrix} h \\ \dot{h} \end{bmatrix}.$$

For the purpose of the analysis, the parameter values $Z_u = -45.004\,\mathrm{m\,rad^{-1}\,s^{-2}}$ and $Z_\alpha = 3.0785\,\mathrm{s^{-1}}$ have been used, which roughly resemble the behaviour of a Stemme S15 motor glider [3].

2.2. Actuator Model

For the comparative study, a second-order linear model of an electric actuator from Meyer-Brügel and Silvestre [3] is considered. The actuator model is defined by:

$$\ddot{u} = \frac{K_t}{J} I, \tag{3}$$

where $K_t = 5.64\,\mathrm{N\,m\,A^{-1}}$ is the motor torque constant, $J = 0.3320\,\mathrm{kg\,m^2}$ is the moment of inertia and I is the actuator current.

2.3. Actuator Control

To track the commanded control surface deflection, the electric actuator is driven by a cascaded servo control law. This structure consists of two proportional controllers: an outer actuator position control loop and an inner actuator speed loop. The outer loop computes the desired rate command based on

$$\dot{u}_c = K_{\dot{u}u}(u_c - u), \tag{4}$$

where $K_{\dot{u}u} = 30\,\mathrm{s^{-1}}$ is the gain for the actuator position control loop. The inner loop then computes the actuator current command based on

$$I = K_{I\dot{u}}(\dot{u}_c - \dot{u}), \tag{5}$$

where $K_{I\dot{u}} = 8\,\mathrm{A\,s\,rad^{-1}}$ is the gain for the actuator velocity control loop. The commanded actuator current I serves as the input to the actuator dynamics.

3. CONTROL APPROACHES

In this section, the control approaches examined in this comparative analysis will be detailed.

3.1. Local Acceleration Control (LAC) Approach

The Local Acceleration Control (LAC) approach, first introduced by Meyer-Brügel and Silvestre [3], is driven by the intention to unify the control design of flight and actuator controllers to achieve aeroelastic control in a potentially extended frequency range and improve robustness as well as disturbance rejection. The concept replaces the "classical" actuator position feedback loop with the feedback of the local acceleration measured at the control surface.

Viewing the complete state-space, comprising flight dynamic states as well as actuator states, the authors showed that feeding back the local acceleration rather than control surface deflection results in feeding back the same system state vector just in different coordinates. In consequence, for any classic state-feedback controller, there exists an analogue LAC based control law yielding the same closed-loop dynamics. Its parameters may be determined from the classical ones using the appropriate state transformation or by comparing the resulting transfer functions.

For the basic example introduced in section 2.1, a cascaded state-feedback structure involving a vertical speed and an altitude control loop is assumed. Combined with the actuator control law equations 4 and 5, the complete feedback law

$$I = K_{I\dot{u}}(K_{\dot{u}u}(K_{u\dot{h}}(K_{\dot{h}h}(h_c - h) - \dot{h}) - u) - \dot{u}) \tag{6}$$

based on the classical position controlled actuators is obtained, where $K_{u\dot{h}}$ and $K_{\dot{h}h}$ denote the vertical speed and altitude control loop gains. Following the LAC approach, the actuator position feedback u is replaced by the (local) acceleration feedback $\ddot{h}$, which results in the corresponding LAC based control law

$$I = K_{I\dot{u}}(K_{\dot{u}\ddot{h}}(K_{\ddot{h}\dot{h}}(K_{\dot{h}h}(h_c - h) - \dot{h}) - \ddot{h}) - \dot{u}). \tag{7}$$

The required parameter relationship

$$K_{\dot{u}\ddot{h}} = \frac{-1}{Z_u} K_{\dot{u}u}, \tag{8}$$

$$K_{\ddot{h}\dot{h}} = -Z_u K_{u\dot{h}} + Z_\alpha, \tag{9}$$

$$K_{\dot{h}h}^{\text{accel}} = \frac{-Z_u K_{u\dot{h}} K_{\dot{h}h}^{\text{class}}}{K_{\ddot{h}\dot{h}}} \tag{10}$$

to achieve the same closed loop dynamics compared to the classical control law is derived in appendix A.

In the following sections, it will be shown that all the above-mentioned control approaches share the outer-loop structure (velocity and altitude control loop) and the actuator rate control loop. Therefore, to facilitate a consistent comparison, the analysis will be restricted to the acceleration control loop generating the actuator rate command. The revised control law for the LAC approach is given by:

$$\boxed{\dot{u}_c = (\ddot{h}_c - \ddot{h}) K_{\dot{u}\ddot{h}}}. \tag{11}$$

The LAC approach will serve as the baseline for the remainder of this work, with all subsequent control approaches designed to match its performance.

3.2. NDI Approach

The NDI approach strives to compensate for the non-linearity of the plant by identifying and inverting a direct relationship between the control input(s) u and a derivative of the variable y to be controlled. Consider the non-linear input-affine system

$$\begin{aligned} \dot{x} &= f(x) + g(x)u \\ y &= h(x). \end{aligned} \tag{12}$$

In the NDI approach, the fundamental principle is to find the r-th time derivative of y, where the time derivative

$$y^{(r)} = a_\nu(x) + B_\nu(x)u \equiv \nu \tag{13}$$

is directly affected by the input u as $B_\nu \neq 0$ [4]. The relation is inverted to obtain

$$u_c = B_\nu^{-1}(x)(\nu_{\text{des}} - a_\nu) \tag{14}$$

which allows to compute u_c from a desired value $\nu_{\text{des}} = y^{(r)}_{\text{des}}$ denoted as *pseudo-control* [4, 5]. Due to the now linear relationship between y and ν, simple linear error control may be employed to achieve a desired closed-loop dynamics.

Although being already linear in nature, the same procedure may be applied to the basic model in section 2.1. Choosing $y = h$ as the controlled variable yields the derivatives

$$\dot{y} = \dot{h} = CAx + \underbrace{CBu}_{=0},$$
$$\ddot{y} = \ddot{h} = CA(\dot{x}) = CA^2x + CABu \equiv \nu, \tag{15}$$

which unveil the second time derivative $\ddot{y} = \ddot{h}$ as the pseudo-control because it is directly impacted by the control input u. Inverting equation 15 yields

$$u_c = (CAB)^{-1}(\ddot{h}_c - CA^2x), \tag{16}$$
$$= \frac{-1}{Z_u}(\ddot{h}_c + Z_\alpha \dot{h}). \tag{17}$$

This control command is realised by a classical actuator. Therefore, in combination with the position control loop, the control law

$$\dot{u}_c = (u_c - u)K_{\dot{u}u},$$
$$\xRightarrow{\text{(eq.17)}} \boxed{\dot{u}_c = \left(\frac{-1}{Z_u}(\ddot{h}_c + Z_\alpha \dot{h}) - u\right) K_{\dot{u}u}}. \tag{18}$$

for the NDI approach formulated in terms of the commanded actuator speed is obtained.

3.3. INDI Approach

The INDI approach builds on the basis of the NDI approach. The INDI approach increases the robustness of the NDI approach by replacing the model-dependent term a_ν in equation 14 with measurements of the $\nu = y^{(r)}$ and current control input u, using the expression [5, 6]

$$a_\nu(x) = \nu - B_\nu u. \tag{19}$$

Inserting the above expression in equation 14 leads to the INDI control law

$$u_c = u + B_\nu^{-1}(x)(\nu_{\text{des}} - \nu) \tag{20}$$

which reflects an incremental change

$$\Delta u = u_c - u = B_\nu^{-1}(x)(\nu_{\text{des}} - \nu) \tag{21}$$

with respect to the current control input u.

Applied to the basic example, where

$$B_\nu = CAB = -Z_u, \tag{22}$$

we obtain

$$u_c = u + \frac{-1}{Z_u}(\ddot{h}_c - \ddot{h}), \tag{23}$$

where $\nu_{\text{des}} = \ddot{h}_c$ and $\nu = \ddot{h}$. The control law for the INDI approach, expressed in terms of the commanded actuator speed, is given by:

$$\dot{u}_c = (u_c - u)K_{\dot{u}u},$$
$$\Rightarrow \boxed{\dot{u}_c = \frac{-1}{Z_u}(\ddot{h}_c - \ddot{h})K_{\dot{u}u}}. \tag{24}$$

From this equation, it becomes evident, that the negative position feedback, which is inherent to practically all actuator controllers, cancels the positive feedback of the actuator position and thereby essentially eliminates the incremental character of the INDI control law. Thus, the INDI command should be interpreted as a direct actuator rate command. This has already been reported by [5]. However, a perfect cancellation would only take place in an ideal scenario and may not be valid under non-ideal conditions, since in practice the required positive feedback must be obtained via an additional sensor, an observation procedure, or processed actuator measurements, and therefore, perfect cancellation cannot be achieved.

3.4. Extended-INDI Approach

The extended-INDI (E-INDI) approach modifies the INDI approach by incorporating actuator dynamics into the control allocation [7]. In this extended approach, the pseudo-control in equation 13 is differentiated again, resulting in

$$\dot{\nu} = \frac{\partial(a_\nu(x) + B_\nu(x)u)}{\partial x}\dot{x} + \frac{\partial(a_\nu(x) + B_\nu(x)u)}{\partial u}\dot{u},$$
$$= A_\nu(x,u)\dot{x} + B_\nu(x)\dot{u}. \tag{25}$$

Here, the state-dependent ($A_\nu \dot{x}$) term is often neglected [5, 7], giving rise to the inversion law

$$\dot{\nu} = B_\nu(x)\dot{u}. \tag{26}$$

Following [7], an arbitrary actuator dynamics may be represented as:

$$\dot{u}(s) = K_{\text{act}} \cdot F_{\text{act}}(s)(u_c - u) \tag{27}$$

which explicitly separates the outer position control loop dynamics (gain K_{act}) from the remaining inner higher-order dynamics. An analogous representation may be chosen for an arbitrary desired dynamics of the pseudo-control, yielding

$$\dot{\nu}(s) = K_\nu \cdot F_\nu(s)(\nu_{\text{des}} - \nu). \tag{28}$$

Inserting equations 27 and 28 in equation 26 results in the control law:

$$u_c = u + F_{\text{act}}(s)^{-1}(B_\nu K_{\text{act}})^{-1}K_\nu F_\nu(s)(\nu_{\text{des}} - \nu) \tag{29}$$

assuming B_ν to be invertible. Otherwise known control allocation methods may be employed on

$(B_\nu K_{\text{act}})$, thus taking the actuator bandwidth directly into account, which is considered a key advantage of E-INDI [7].

From the second-order actuator model, along with its cascaded servo controller described in equations 3, 4 and 5, it can be deduced that

$$K_{\text{act}} = K_{\dot{u}u}, \tag{30}$$

$$F_{\text{act}} = \frac{K_{\dot{u}}}{s + K_{\dot{u}}}, \tag{31}$$

where $K_{\dot{u}} = {}^{K_t K_{I\dot{u}}}/{}_J$. Assuming the desired pseudo-control dynamics

$$\nu(s) = \frac{\omega_0^2}{s^2 + 2\zeta\omega_0 s + \omega_0^2}\nu_{\text{des}}(s) \tag{32}$$

to be of second-order as well, we obtain analogously

$$F_\nu(s) = \frac{2\zeta\omega_0}{s + 2\zeta\omega_0}, \tag{33}$$

$$K_\nu = \frac{\omega_0}{2\zeta}. \tag{34}$$

Inserting equations 30, 31 as well as the expression equation 22 for B_ν in equation 29 results in the control law

$$u_c = u + \frac{s + K_{\dot{u}}}{K_{\dot{u}}}(-Z_u K_{\dot{u}u})^{-1} K_\nu F_\nu(s)(\ddot{h}_c - \ddot{h}). \tag{35}$$

Again, the control command u_c is subject to the actuator position control loop equation 4 which allows to formulate the control law in terms of commanded actuator speed:

$$\begin{aligned} &\dot{u}_c = (u_c - u)K_{\dot{u}u}, \\ \Rightarrow &\boxed{\dot{u}_c = \frac{-1}{Z_u}\left(\frac{s + K_{\dot{u}}}{K_{\dot{u}}}\right) K_\nu F_\nu(\ddot{h}_c - \ddot{h})}. \end{aligned} \tag{36}$$

3.5. ANDI Approach

The *Actuator* NDI approach (ANDI) [8] is similar to the extended-INDI approach, however, it puts on new theoretical grounds, providing insight into the implicit assumptions underlying the INDI control approach and the effect of actuator dynamics on control performance. The ANDI control law represents an exact inversion law, which is obtained by applying NDI not only to the flight dynamics plant, but also to the complete system including actuator dynamics. The system output equation 13 is differentiated again resulting in

$$\dot{\nu} = A_\nu(x, u)\dot{x} + B_\nu(x)\dot{u}. \tag{37}$$

Assuming similar actuator dynamics as equation 27 and similar pseudo-control as equation 28, the above inversion law results in the control law:

$$u_c = u + F_{\text{act}}(s)^{-1}(B_\nu K_{\text{act}})^{-1}(K_\nu F_\nu(s)(\nu_{\text{des}} - \nu) - A_\nu \dot{x}). \tag{38}$$

Comparing this with the E-INDI control law, the difference is made by taking the state dependent term $A_\nu \dot{x}$ into account. Applied to the basic example, where

$$A_\nu \dot{x} = CA^2\dot{x} = -Z_\alpha \ddot{h} \tag{39}$$

the ANDI approach results in the control law

$$u_c = u + \left(\frac{s + K_{\dot{u}}}{K_{\dot{u}}}\right)\frac{-1}{Z_u K_{\dot{u}u}}(K_\nu F_\nu(\ddot{h}_c - \ddot{h}) + Z_\alpha \ddot{h}). \tag{40}$$

The control law formulated in terms of the commanded actuator speed is given by:

$$\begin{aligned} &\dot{u}_c = (u_c - u)K_{\dot{u}u}, \\ \Rightarrow &\boxed{\dot{u}_c = \frac{-1}{Z_u}\left(\frac{s + K_{\dot{u}}}{K_{\dot{u}}}\right)\left[K_\nu F_\nu(\ddot{h}_c - \ddot{h}) + Z_\alpha \ddot{h}\right]}. \end{aligned} \tag{41}$$

4. RESULTS

This results section is structured to first evaluate each control approach under ideal, nominal conditions. Subsequently, a robustness analysis of the approaches will be presented, in which the impact of sensor dynamics, rate dynamics and model parameter uncertainties are investigated.

4.1. Nominal Case

Control Approach	Control Law
LAC	$\dot{u}_c = (\ddot{h}_c - \ddot{h})K_{\dot{u}\ddot{h}}$
NDI	$\dot{u}_c = \frac{-1}{Z_u}(\ddot{h}_c - (-Z_\alpha \dot{h} - Z_u u))K_{\dot{u}u}$
INDI	$\dot{u}_c = \frac{-1}{Z_u}(\ddot{h}_c - \ddot{h})K_{\dot{u}u}$
E-INDI	$\dot{u}_c = \frac{-1}{Z_u}\left(\frac{s+K_{\dot{u}}}{K_{\dot{u}}}\right) K_\nu F_\nu(\ddot{h}_c - \ddot{h})$
ANDI	$\dot{u}_c = \frac{-1}{Z_u}\left(\frac{s+K_{\dot{u}}}{K_{\dot{u}}}\right)\left[K_\nu F_\nu(\ddot{h}_c - \ddot{h}) + Z_\alpha \ddot{h}\right]$

TAB 1. Overview of the control approaches and their corresponding control laws

The control laws for the basic example derived in the previous sections are summarised in table 1. Figure 1 shows the corresponding block diagrams of the complete control structures. Comparing the equations, the following conclusions may be drawn for an ideal scenario:

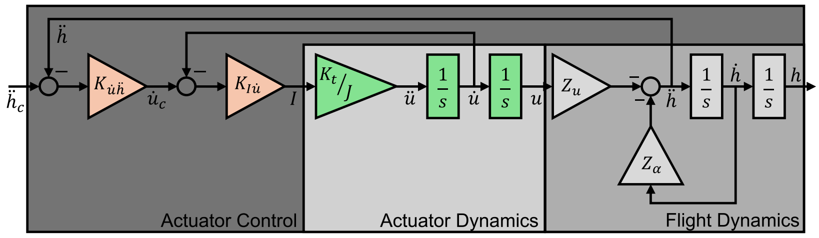

(a) LAC Block Diagram

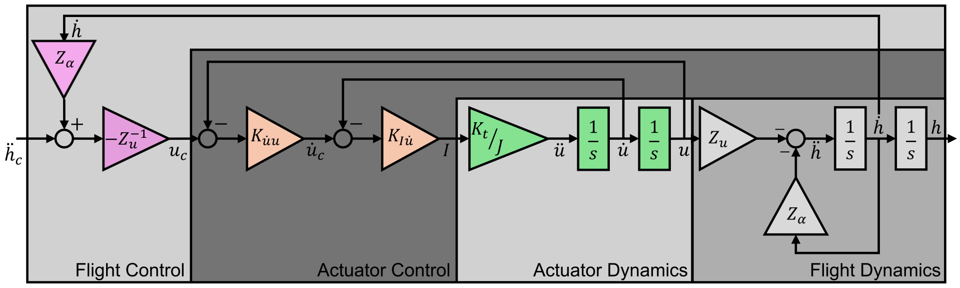

(b) NDI Block Diagram

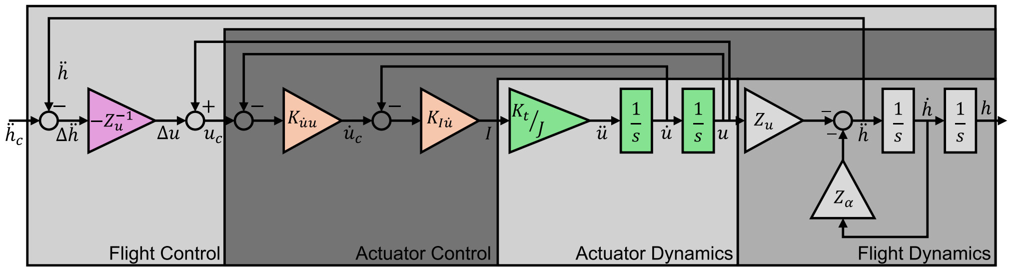

(c) INDI Block Diagram

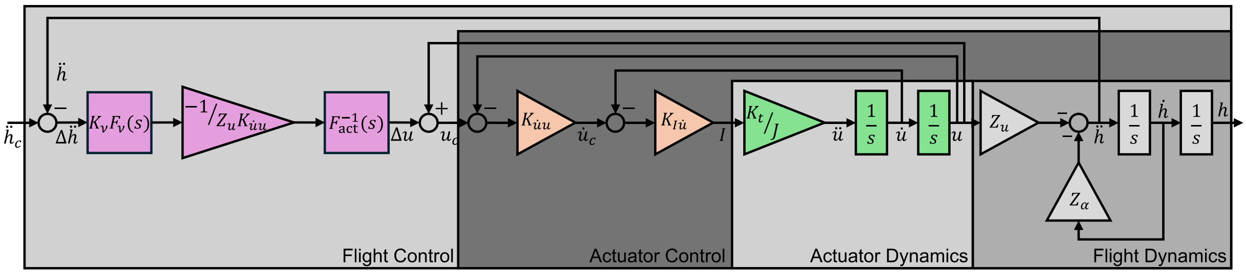

(d) E-INDI Block Diagram

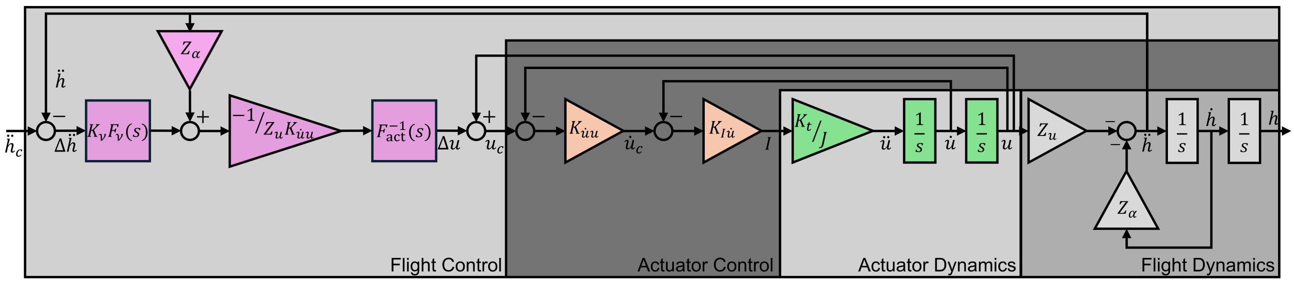

(e) ANDI Block Diagram

FIG 1. Comparison of block diagrams for the complete control structures

1) The LAC and INDI approach result in the same control law if the value

$$K_{\dot{u}\ddot{h}} = \frac{-1}{Z_u} K_{\dot{u}u} \tag{42}$$

is chosen for the LAC gain.

2) Both, the LAC and the INDI approach resemble the NDI control law exactly, as long as a perfect model is used for the NDI, since the term $(-Z_\alpha \dot{h} - Z_u u)$ evaluates to $\ddot{h}$ according to equation 1.

3) A significant advantage of E-INDI (and also ANDI) over the INDI and NDI approaches lies in the ability to explicitly define a desired pseudo-control dynamics, thereby essentially inverting and modifying the actuator dynamics. The LAC approach also offers this capability, as the unified design allows

for the modifications of the internal actuator control loop gains directly. By comparing the LAC control law

(43) $$\ddot{u} = K_{\dot{u}}(K_{\dot{u}\ddot{h}}\Delta\ddot{h} - \dot{u})$$

with the E-INDI control law

(44)
$$\ddot{u} = K_{\dot{u}}\left(\frac{-1}{Z_u}\left(\frac{s+K_{\dot{u}}}{K_{\dot{u}}}\right)K_\nu\left(\frac{2\zeta\omega_0}{s+2\zeta\omega_0}\right)\Delta\ddot{h} - \dot{u}\right)$$

at the $\ddot{u}$-level in the frequency domain, it can be observed that the two control laws become equivalent by choosing the LAC gains as

(45) $$K_{\dot{u}} = 2\zeta\omega_0$$

(46) $$K_{\dot{u}\ddot{h}} = \frac{-K_\nu}{Z_u}.$$

4) The ANDI approach is set apart from the other approaches by considering and compensating for the state-dependent influence. As an exact inversion law accounting for state-dependent influence as well as the actuator dynamics, it is the only approach able to follow the pseudo-control command exactly.

These findings shall also be demonstrated by a numerical simulation, using a 4th order Runge-Kutta method with a sample time of $1 \times 10^{-5}\,\mathrm{s}$, which will resemble an ideal continuous system behaviour with negligible errors. Note that the non-causal term $({s+K_{\dot{u}}}/{K_{\dot{u}}})$ in equations 36 and 41 has been approximated by extending this term with a low-pass filter with a time constant $\tau = \frac{1}{1500}\,\mathrm{s}$. Additionally, for the purpose of this comparative study and to match the performance of the NDI/INDI approach, the desired actuator dynamics is selected to match the existing actuator dynamics, resulting in $K_\nu = K_{\text{act}}$ and $F_\nu = F_{\text{act}}$.

Figure 2 presents the system response to a step command in vertical acceleration ($\nu_{\text{des}} = \ddot{h}_{\text{c}}$) for the five control approaches, alongside the reference model, represented by equation 32. Analysis of the results reveals the expected separation between the different approaches. Under nominal conditions, the ANDI approach performs identically to the reference model. Additionally, the LAC, E-INDI, INDI and NDI approaches also exhibit identical behaviour to each other, which is consistent with the equations outlined above. In particular, the ANDI approach achieves perfect tracking of the commanded value, whereas the other approaches display a settling error, which is caused by the missing compensation of the state-dependent influence.

Figure 3 illustrates the system response to a step command in vertical acceleration, comparing the results of the three approaches for a choice of pseudo-control dynamics

$$K_\nu = 47.0\,\mathrm{s}^{-1}, \quad F_\nu = \frac{212.8}{s+212.8}.$$

different from the original actuator dynamics. The required LAC gains

$$K_{\dot{u},\text{mod}} = 2\zeta\omega_{0,\text{des}} = 212.8\,\mathrm{s}^{-1}\,\mathrm{rad}^{-1}$$
$$K_{\dot{u}\ddot{h},\text{mod}} = \frac{-1}{Z_u}\cdot\frac{\omega_{0,\text{des}}^2}{K_{\dot{u},\text{mod}}} = 1.04\,\mathrm{rad\,s\,m}^{-1}.$$

have been determined according to equations 45 and 46. For comparison, the response with the original actuator frequency is also included and labelled as the reference lines. The figure depicts that all three approaches: LAC, E-INDI and ANDI, successfully modify and achieve the desired higher actuator frequency. This is characterised by the faster rise time of all approaches compared to their respective reference responses.

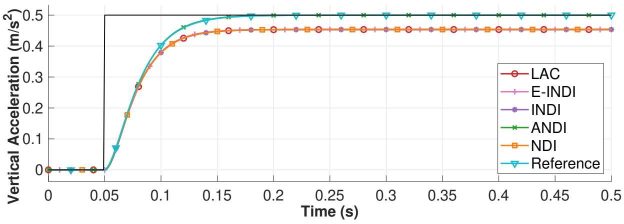

FIG 2. System response to a step command in vertical acceleration

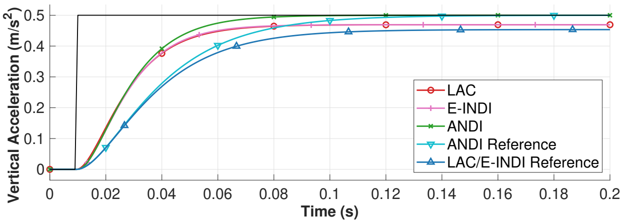

FIG 3. Step response for the LAC, E-INDI and ANDI approaches with actuator frequency $\omega_{0,\text{des}} = 100\,\mathrm{rad\,s}^{-1}$

4.2. Real Case

In the previous section it has been shown for an idealised scenario, that the LAC, NDI, INDI and E-INDI approaches converge to the same control law, if parameters are adjusted appropriately. However, the following idealising assumptions may not hold in reality, leading to different performance:

1) The equivalency between LAC and the incremental control approaches relies on the effect, that the positive feedback of u inherent to the incremental command cancels the negative feedback of u within the actuator position control loop (see equation 4). Thereby, the actuator position control is essentially eliminated, which is also the concept behind LAC. In practice however, the positive feedback being the basis of incremental control, is to be

acquired by the flight control unit by means of an independent second position sensor, a kind of observation procedure, based on the command values from previous time steps or obtaining a processed version of the actuator internal measurements from the actuator control unit. In either case, perfect cancellation will not occur.

2) In a real implementation, both, flight control and actuator control are discretised systems, hence the idealised continuous representation of the control laws will no longer hold. This is especially true for the FCL part, since flight controllers usually work with significant lower sampling rates compared to actuator control.
3) The non-causal transfer function F_{act}^{-1} involved in the E-INDI and ANDI control laws has to be approximated by extending the term with a low-pass filter, involving numerical differentiation. The pole-zero cancellation for $K_{\dot{u}}$ will not take place exactly and the transfer functions F_{ν} and F_{act} may not be combined to yield a causal relationship depending on the type of control allocation involved.
4) The model assumption underlying the NDI approach may not match the real behaviour of the plant. Hence, there is a discrepancy

$$\ddot{h} \neq -Z_{\alpha}^{\text{model}}\dot{h} - Z_{u}^{\text{model}}u \tag{47}$$

due to model uncertainties, making the NDI control law diverge from the approaches. This is a well-known drawback of the NDI approach causing robustness issues, which has been overcome by the INDI approach [5].

The possible impact of these real-world effects will be assessed in the following sections.

4.2.1. Effect of Sensor Model

In this subsection, the effect of an imperfect cancellation of the actuator position feedback by the incremental control approaches (INDI, E-INDI and ANDI) is analysed. To assess these effects, it is assumed that the basis value of the control increment Δu is obtained by the FCL using a second independent sensor for the actuator position. A simplified sensor model is implemented, as these approaches use an additional feedback of the actuator position, as seen in their respective block diagrams in figure 1. The sensor model is depicted in the block diagram in figure 4. The model incorporates a first-order low-pass filter with a cut-off frequency f_c to represent the sensor dynamics, sensor delay, sensor offset and measurement noise. It should be noted that the sensor within the actuator that measures the actuator position would also contribute to the overall sensor impact, as the impact is caused by the difference of these two sensor signals, the source of the error is less relevant. For the sake of a more transparent analysis, the error effects will therefore, be summarised in the FCL position sensor, while the actuator position sensor within the actuator control loop is assumed ideal.

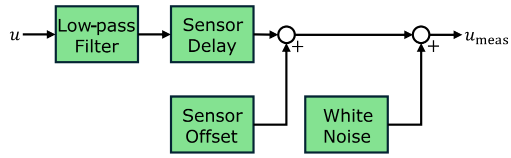

FIG 4. Sensor model block diagram

Sensor Dynamics

In the presented sensor model, a first-order low-pass filter

$$H(s) = \frac{1}{\frac{1}{2\pi f_c}s + 1} \tag{48}$$

with a cut-off frequency f_c is used to model the sensor dynamics. To analyse the impact of the cut-off frequency on the control approaches, it is varied between $2\,\mathrm{Hz}$ and $1000\,\mathrm{Hz}$. The system responses for the INDI, E-INDI and ANDI control approaches are shown in figures 5 and 6. As illustrated in figure 5, the INDI and E-INDI approaches exhibit identical behaviour with regard to filter cut-off frequency. At higher cut-off frequencies, the INDI and E-INDI approaches the performance of the LAC approach, while the ANDI approach coincides with the reference model. From the figures it is also observed that the cut-off frequency has minimal influence on the system's initial response. However, reducing the cut-off frequency leads to a significant increase in the settling time and a noticeable increase in the steady-state error of the pseudo-control response.

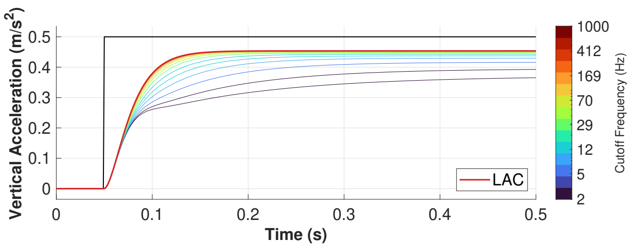

FIG 5. Step response for INDI and E-INDI approaches with increasing cut-off frequency

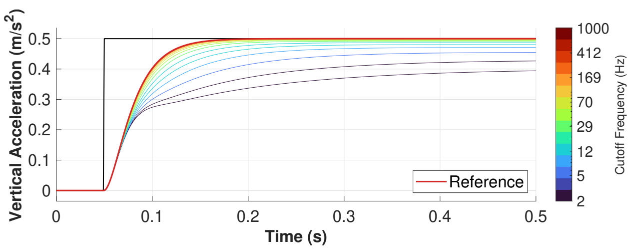

FIG 6. Step response for ANDI approaches with increasing cut-off frequency

Sensor Delay

Figures 7 and 8 illustrate the effects of the sensor delay on the system response for the INDI, E-INDI and ANDI control approaches. In the simulations, the sensor delay is varied from $0\,\mathrm{ms}$ to $100\,\mathrm{ms}$. Similar to what is observed in the case of the first-order filter, figure 7

©2026

shows that the INDI and E-INDI approaches exhibit identical behaviour. For both the INDI and E-INDI approaches, the zero sensor delay case matches the system response of the LAC approach (which is not affected by the sensor errors), while in the case of the ANDI approach, this same case coincides with the response of the reference model. Similar to the effect of the sensor dynamics, the figures reveal that, for all three approaches, increasing the sensor delay introduces an additional steady-state error. Furthermore, the introduction of sensor delay additionally causes an oscillation tendency, which has not been observed for pure sensor dynamics. It is also observed that, in all three approaches, the addition of a sensor delay on the actuator position feedback, does not result in a response delay in the system. It is noted here, that for the ANDI approach, a sensor delay of $30\,\mathrm{ms}$ yields a steady-state error of the same magnitude as the deviation relative to the reference model shown by the INDI/E-INDI approaches.

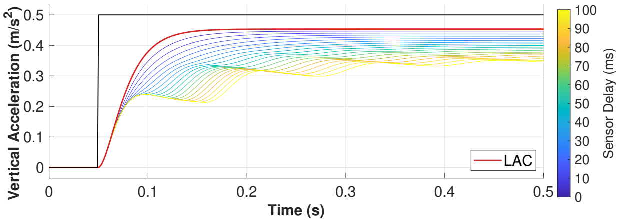

FIG 7. Step response for INDI and E-INDI approaches with increasing sensor delay

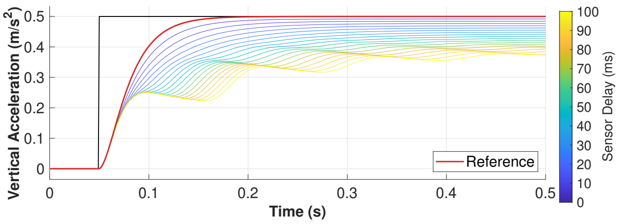

FIG 8. Step response for ANDI approaches with increasing sensor delay

Sensor Offset

In this analysis, the sensor offset is defined as a percentage of the maximum actuator angle measurement range (defined here as $\pm 30°$). The offset is varied between 0% and 1% of this range and the resulting system responses are shown in figures 9 and 10. The figures indicate that sensor offset only affects the steady-state response of the system. With an increasing sensor offset, the system response shifts parallel, leading to a higher steady-state error across all three control approaches: INDI, E-INDI and ANDI. Notably, in the zero-offset case, both INDI and E-INDI match the LAC system response, whereas the zero-offset ANDI coincides with the reference model.

Sensor Noise

In the sensor model introduced above, the white sensor noise is modelled using a random number generator, which adds uncorrelated random values upon each time sample in the quasi-continuous simulation running at $100\,000\,\mathrm{Hz}$. Similar to the sensor offset, the maximum sensor noise level is defined as a percentage of the maximum angle measurement range and is varied between 0% and 1%. The system responses to a step input in vertical acceleration under varying noise levels are presented in figures 11 and 12. The results indicate that, similar to the sensor offset, sensor noise does not affect the dynamic response of the system in all three control approaches. However, at higher noise levels, a noticeable fluctuation around the steady-state value is observed. For the zero-noise case, both INDI and E-INDI responses match the LAC system response, while the zero-noise ANDI response coincides with the reference model.

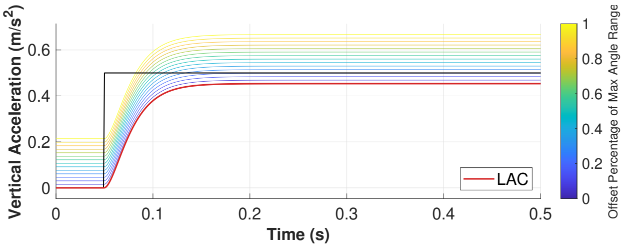

FIG 9. Step response for INDI and E-INDI approaches with increasing sensor offset

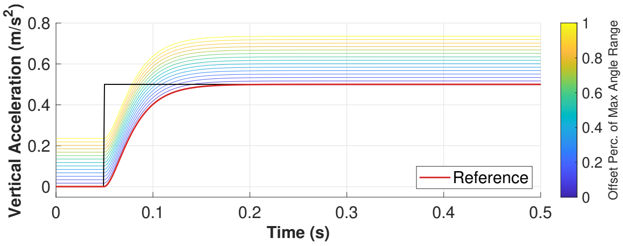

FIG 10. Step response for ANDI approaches with increasing sensor offset

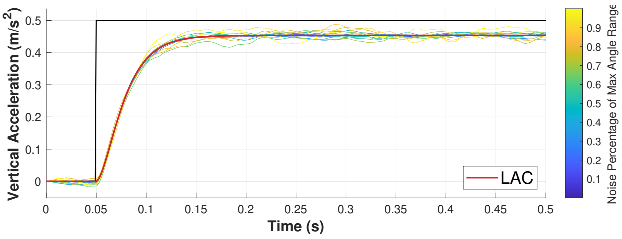

FIG 11. Step response for INDI and E-INDI approaches with increasing sensor noise

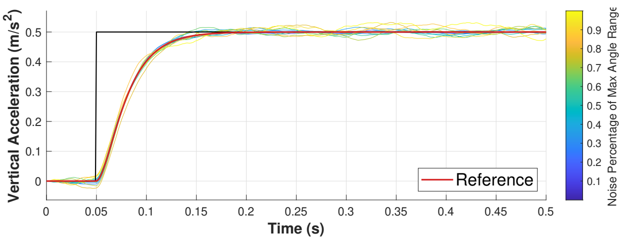

FIG 12. Step response for ANDI approaches with increasing sensor noise

4.2.2. Effect of Rate Dynamics

Until now, only the quasi-continuous system behaviour has been assessed using a higher-order integration method and very fast sample rates. However, real-world implemented control systems are inherently discrete. Additionally, it is common for the actuator controller to operate at a considerably higher frequency than the flight controller. In the following section, the impact of the system discretisation is analysed, with a focus on the effects of differing update rates between the actuator controller and the flight controller. For this analysis, the discrete actuator controller is set to $10\,000\,\mathrm{Hz}$, whilst the flight controller update frequency is varied. According to the LAC approach, the acceleration feedback replaces the actuator position control, which is implemented on the actuator control unit (ACU). Therefore, the results for this approach are not affected by the flight controller update rate.
As discussed in point 3) above, for the E-INDI and ANDI approaches, the inverse of the actuator transfer function F_{act} is implemented by extending the inverse with a first-order low-pass filter. Since this filter has to be realised in a discrete system, the maximum cut-off frequency is limited by the sampling frequency of the flight control laws. In this study, a zero-order hold method has been used to transform the continuous transfer function into the discrete domain. Assuming a maximum tolerable discretisation error of 1% in terms of the Mean Absolute Percentage Error(MAPE), a required ratio of ${F_{\text{cut-off}}}/{F_{\text{sample}}} > 16.8$ can be derived.

Assuming a flight controller frequency of $100\,\mathrm{Hz}$, this ratio yields a filter cut-off frequency of approximately $6\,\mathrm{Hz}$. The results shown in figure 13, indicate that the E-INDI and ANDI approaches are able to reach their steady-states. However, these approaches exhibit significantly larger overshoots and longer settling times compared to the other control approaches analysed. From the figure 13, it can also be observed that the discretisation introduces a small delay in the NDI and INDI approaches. However, this delay does not affect the overall system stability. While stability is maintained, the discretisation leads to a noticeable steady-state error (SSE) relative to the continuous system. The figures presented above also indicate a small delay in the LAC approach, however, this delay does not influence the SSE relative to the continuous system and therefore, the LAC approach remains robust to the discretisation of the flight controller.

The observed effects in the figure above can be attributed to two distinct discretisation phenomena. The first arises from the cut-off frequency of the filter in the E-INDI and ANDI approaches. The second effect stems from the delay introduced by the update rate in the positive feedback signal of the actuator position. To separate these factors, two parameter studies were conducted using the E-INDI approach.

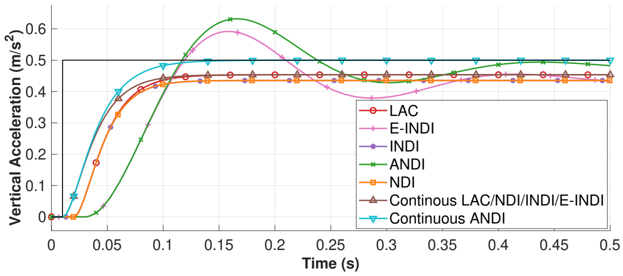

FIG 13. Step response for flight controller update frequency set to 100 Hz and filter cut-off frequency set to 6 Hz

First, to highlight the effects of varying the filter cut-off frequency, the flight controller was set to have an update rate of $4000\,\mathrm{Hz}$ and the filter cut-off frequency was varied from $2\,\mathrm{Hz}$ to $4000\,\mathrm{Hz}$. Figure 14 illustrates the influence of the filter's cut-off frequency on the system response compared to the ideal continuous response (solid red line). At lower cut-off frequencies, the system exhibits a significant deviation from the continuous response, which is characterised by longer settling times and large overshoots. This is because the filter frequency approaches the actuator dynamics, thus the introduced phase delay affects the control response. As the cut-off frequency increases, the system response converges to the ideal response, with reduced overshoots and faster settling times. However, increasing the filter frequency further introduces deviations to the ideal profile and an oscillatory response again, as soon as the cut-off frequency approaches the sampling frequency. This suggests there is an optimal range of cut-off frequencies where the system's response most closely resembles the continuous response. To quantitatively assess performance, MAPE was calculated for each cut-off frequency. A range of filter frequencies of $18.5\,\mathrm{Hz}$ to $1600\,\mathrm{Hz}$ was determined where the MAPE values are below 5%. The lower boundary corresponds to a factor of 216 and the upper boundary corresponds to a factor of 2.5 relative to the flight controller update frequency. This analysis highlights that the choice of filter time constant plays a critical role for the E-INDI and ANDI approaches, as it can strongly influence the system performance and stability. In real scenarios, the possible range to select the filter frequency is expected to be rather small, since flight controller update rates are usually chosen in accordance with the flight mechanical eigenvalues and the actuator dynamics are typically much faster. More sophisticated discretisation methods may weaken this constraint, however, the principal problem remains.

The second parameter study concerns the update delay of the reference for the incremental control commands. To isolate this impact and distinguish it from the effect of the previously discussed low-pass filter, the E-INDI control law has been modified to directly combine the transfer functions of the desired pseudo-control dynamics F_{ν} and the inverse of the real ac-

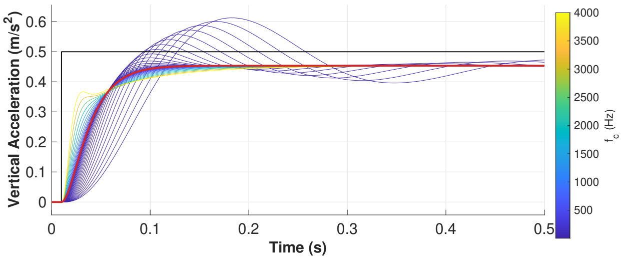

FIG 14. Step response for E-INDI approach with increasing filter cut-off frequency

tuator dynamics F_{act}^{-1} (as previously noted, this might not always be possible beyond the simple example treated here, depending on the type of control allocation involved). This results in a proper transfer function that can be directly realised, eliminating the need for the additional low-pass filter. However, it should be noted that this modification cannot be applied to the ANDI approach due to the presence of the additional state feedback(CA^2x) in its structure. Figure 15 details the results of a parameter study in which the flight controller update frequency is varied between $10\,\mathrm{Hz}$ and $4000\,\mathrm{Hz}$. The solid red line in the figure represents the ideal continuous response of the E-INDI approach. As the flight controller update rate is reduced, a significant delay and deviation is observed compared to the continuous system response. Additionally, a SSE is introduced in the pseudo-control response, which increases for lower FCL sample rates. Furthermore, due to the small steps arising in the feedback signal due to the discretisation, higher frequent signal content is introduced in the response. This disturbance yields the sample rate synchronous oscillation cycles observed, which should not be misunderstood as a dynamic oscillation tendency. A minimum flight controller frequency of $400\,\mathrm{Hz}$ is required to achieve a MAPE below 5%, indicating the lower bound for acceptable tracking accuracy and stability.

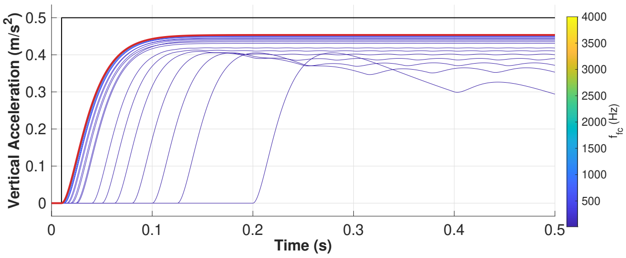

FIG 15. Step response for E-INDI approach with increasing flight controller update frequency

4.2.3. Effect of Model Parameter Variation

In the following section, the robustness of the control approaches is evaluated with respect to variations in model parameters. In this analysis, the two flight dynamics parameters Z_u and Z_α have been varied. The controllers originally designed for the nominal case have been used without modification to control the modified systems.

Figures 16 and 17 show the system response to a step input in vertical acceleration for the five control approaches: LAC, NDI, INDI, E-INDI and ANDI, under varying flight dynamics parameters. From both figures, it is evident that the NDI approach is highly susceptible to model parameter variations. Z_u acts as an additional gain that effectively increases K_ν, which mainly influences the initial response of the system. A variation of Z_α represents a change in state influence. Z_α enters the model-based calculation of $\ddot{h}$ in NDI. As a result, the steady-state tracking error remains more sensitive to Z_α in NDI. From both figures, it is also observed that model parameter variations lead to a variation of the steady-state response, however, the system remains stable.

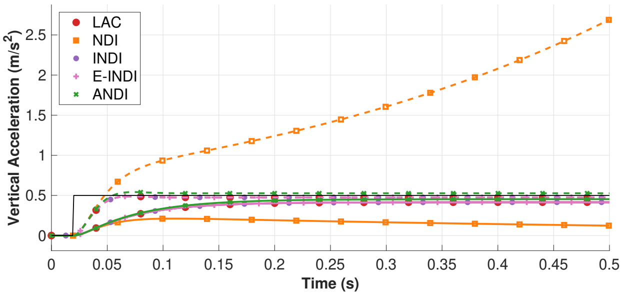

FIG 16. System Response to a step input in vertical acceleration for Z_u variation. Solid lines correspond to $Z_u \cdot 0.5$ and dashed lines correspond to $Z_u \cdot 2$

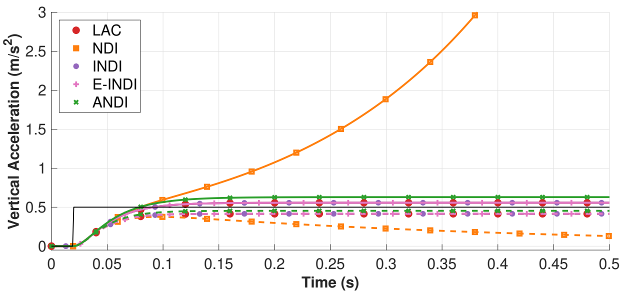

FIG 17. System Response to a step input in vertical acceleration for Z_α variation. Solid lines correspond to $Z_\alpha \cdot 0.5$ and dashed lines correspond to $Z_\alpha \cdot 2$

5. CONCLUSION

For a simple, linear example, we have shown that the NDI, INDI, E-INDI and LAC yield the same control law when parameters are chosen appropriately. This is remarkable since the approaches originate from very different perspectives - while the LAC approach is derived from a linear assessment involving a basis change in the unified state-space comprising actuator and flight dynamics states, the other control approaches are driven by the intention to compensate for non-linear behaviour of the control plant and improve control allocation. This result suggests that the LAC approach shares the intrinsic ability to compensate non-linear system behaviour. However, this has to be confirmed by exploring more sophisticated models in the non-linear domain.

The equivalency between NDI and the other approaches holds only as long as an ideal model is used for the inversion. The point made by the INDI method is to replace the model-based computation of the actual pseudo-control by direct measurements of input and state derivatives, which is known to improve robustness and disturbance suppression significantly. The same advantage is shared not only by E-INDI and ANDI but notably also by LAC.

Since the NDI and INDI approaches do not account for actuator dynamics, they follow the pseudo-control reference with the natural dynamics of the actuators. This flaw is tackled by E-INDI, which allows us to specify a desired pseudo-control dynamics independent of the natural actuator dynamics, which is especially useful, if multiple actuators with different characteristics are involved in the control allocation. This is essentially realised by inverting the natural actuator dynamics and replacing it with a desired one. We have shown that the same effect may be achieved with LAC, but since it is an actuator control law, the gains can be changed directly.

The ANDI approach, however, sets itself apart, since it represents an exact inversion law comprising also the actuator dynamics. This is not considered by classical NDI and therefore, introduces a flight state influence on the pseudo-control dynamics for all other approaches.

The observed equivalency between (E-)INDI and LAC relies on the fact that all INDI based approaches - owing to their incremental nature - involve a positive feedback of the actuator position. On the other hand, known actuator controllers compensate a position error, which involves a negative feedback of the actuator position. Although realised in different hardware units, both counteracting feedback loops would ideally cancel. However, the elimination of the actuator position feedback is exactly the key feature of LAC. Therefore, the LAC approach may also be understood as "E-INDI across hardware units" [5] and vice versa.

For real implementations, it makes a difference whether the effect is achieved by inversion (implemented in the FCC) or a direct modification of actuator control (implemented in the ACU). Our study highlights that any deviation between the counter-acting signals which will arise from imperfect measurements, estimations or communication delay, will deteriorate the control performance. Asynchronism due to measurement or processing delays has been identified most critical for stability, while stationary or random errors will decrease accuracy but leave system dynamics unaffected. Furthermore, the inversion of actuator dynamics requires non-causal behaviour to be approximated by filters. We have shown that contradicting constraints leave a very narrow band to choose those filter frequencies from, thus posing high requirements on the FCL sampling rate.

Depending on the type of actuation system, there might be some inner dynamics resulting from physical effects rather than being imposed by actuator control or an adaptation of actuator control is not justifiable for commercial reasons. In those cases, (E-)INDI and ANDI are viable and promising options, as long as update rates and delays are planned with care. However, since all these incremental approaches do effectively control actuator dynamics and are active in the respective higher frequency band, it makes most sense to implement them in an actuator control unit, providing lower lag times and adequate sample rates. Furthermore, as it is questionable to invert a dynamics, which had been intentionally designed beforehand, any attempt to should be made to modify the actuator controller directly, no matter if we call it LAC or E-INDI across hardware units.

Contact address:

sutej.singh@tu-berlin.de

References

[1] Flávio J. Silvestre and Robert Luckner. Experimental Validation of a Flight Simulation Model for Slightly Flexible Aircraft. *AIAA Journal*, 53(12):3620–3636, 2015. DOI: 10.2514/1.j054023.

[2] Flávio J. Silvestre, Antônio B. Guimarães Neto, Rafael Mendes Bertolin, Roberto Gil Annes da Silva, and Pedro Paglione. Aircraft Control Based on Flexible Aircraft Dynamics. *Journal of Aircraft*, 54(1):262–271, Jan. 2017. ISSN: 1533-3868. DOI: https://doi.org/10.2514/1.C033834.

[3] Wolfram Meyer-Brügel and Flávio J. Silvestre. Unified Control of Flight Dynamics and Actuators Using Local Accelerations. *Journal of Guidance, Control, and Dynamics*, 2024. DOI: https://doi.org/10.2514/1.G007860.

[4] Brian L. Stevens, Frank L. Lewis, and Eric N. Johnson. *Aircraft Control and Simulation*. Wiley, Hoboken, NJ, third edition edition, 2016. ISBN: 978-1-118-87099-0.

[5] Agnes Steinert, Stefan Raab, Simon Hafner, Florian Holzapfel, and Haichao Hong. From fundamentals to applications of incremental nonlinear dynamic inversion: A survey on INDI – part I. *Chinese Journal of Aeronautics*, page 103553, Apr. 2025. ISSN: 1000-9361. DOI: https://doi.org/10.1016/j.cja.2025.103553.

©2026

[6] Fabian Grondman, Gertjan Looye, Richard O. Kuchar, Q Ping Chu, and Erik-Jan Van Kampen. Design and flight testing of incremental nonlinear dynamic inversion-based control laws for a passenger aircraft. In *2018 AIAA Guidance, Navigation, and Control Conference, January 2018, Kissimmee, Florida*. American Institute of Aeronautics and Astronautics, January 2018. DOI: https://doi.org/10.2514/6.2018-0385.

[7] Stefan A. Raab, Jiannan Zhang, Pranav Bhardwaj, and Florian Holzapfel. Consideration of control effector dynamics and saturations in an extended indi approach. In *AIAA Aviation 2019 Forum, June 2019, Dallas Texas*. American Institute of Aeronautics and Astronautics, June 2019. DOI: https://doi.org/10.2514/6.2019-3267.

[8] Rasmus Steffensen, Agnes Steinert, and Ewoud J. J. Smeur. Nonlinear Dynamic Inversion with Actuator Dynamics: An Incremental Control Perspective. *Journal of Guidance, Control, and Dynamics*, 46(4):709–717, April 2023. ISSN: 1533-3884. DOI: https://doi.org/10.2514/1.G007079.

Appendix

A. LAC DERIVATION

The difference between the classical approach and the LAC approach is visualised in figure 18.

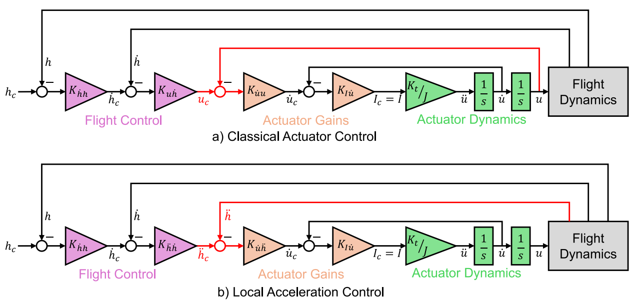

FIG 18. Block diagrams of the classical (a) and LAC (b) approaches, adapted from [3]

The LAC approach has been designed to match the performance of the classical control approach. For the design of the LAC approach Meyer-Brügel and Silvestre formulated the transfer functions for both approaches and compared the terms to calculate the controller gains for the LAC approach [3]. For the classical approach, the transfer function $G^{\text{class}}_{hh_c}(s)$ is defined as:

(49)
$$G^{\text{class}}_{hhc} = -\frac{Z_u K_h}{\left(\begin{array}{r} s^4 + (Z_\alpha + K_{\dot u})s^3 + (Z_\alpha K_{\dot u} + K_u)s^2 \\ + (K_u Z_\alpha - Z_u K_{\dot h})s - Z_u K_h \end{array}\right)},$$

where

$$K_{\dot u} = \frac{K_t}{J} K_{I\dot u}, \quad K_u = K_{\dot u} K_{\dot u u},$$

$$K_{\dot h} = K_u K_{u\dot h}, \quad K_h = K_{\dot h} K^{\text{class}}_{\dot h h},$$

$K_{u\dot h} = 0.01\,\mathrm{rad\,s\,m^{-1}}$ and $K^{\text{class}}_{\dot h h} = 10\,\mathrm{s^{-1}}$. For the LAC approach, the transfer function is expressed as:

(50)
$$G^{\text{accel}}_{hhc} = -\frac{Z_u K_h}{\left(\begin{array}{r} s^4 + (Z_\alpha + K_{\dot u})s^3 + (Z_\alpha K_{\dot u} - Z_u K_{\ddot h})s^2 \\ + (Z_u K_{\dot h})s - Z_u K_h \end{array}\right)},$$

where

$$K_{\dot u} = \frac{K_t}{J} K_{I\dot u}, \quad K_{\ddot h} = K_{\dot u} K_{\dot u \ddot h},$$
$$K_{\dot h} = K_{\ddot h} K_{\ddot h \dot h}, \quad K_h = K_{\dot h} K^{\text{accel}}_{\dot h h}.$$

When comparing the transfer functions of the classical approach (Eq. 49) and the LAC approach (Eq. 50), the differences lie in the zeroth-, first-, and second-order terms of the transfer function denominator. Equating the second-order terms, the following feedback gain $K_{\dot u \ddot h}$ is determined:

$$K_{\dot u} Z_\alpha - Z_u K_{\ddot h} = Z_\alpha K_{\dot u} + K_u,$$
$$\Rightarrow -Z_u K_{\dot u} K_{\dot u \ddot h} = K_{\dot u} K_{\dot u u},$$
(51)
$$\Rightarrow \boxed{K_{\dot u \ddot h} = -\frac{1}{Z_u} K_{\dot u u}}.$$

The feedback gain $K_{\ddot h \dot h}$ is obtained by equating the first-order terms and inserting equation 51 as follows:

$$-Z_u K^{\text{accel}}_{\dot h} = K_u Z_\alpha - Z_u K^{\text{class}}_{\dot h},$$
$$\Rightarrow K^{\text{accel}}_{\dot h} = K^{\text{class}}_{\dot h} - K_u \frac{Z_\alpha}{Z_u},$$
$$\Rightarrow K_{\dot u} K_{\dot u \ddot h} K_{\ddot h \dot h} = K_{\dot u} K_{\dot u u} K_{u\dot h} - K_{\dot u} K_{\dot u u} \frac{Z_\alpha}{Z_u},$$
$$\xrightarrow{(eq.51)} \frac{-1}{Z_u} K_{\dot u u} K_{\ddot h \dot h} = K_{\dot u u} K_{u\dot h} - K_{\dot u u} \frac{Z_\alpha}{Z_u},$$
(52)
$$\Rightarrow \boxed{K_{\ddot h \dot h} = -Z_u K_{u\dot h} + Z_\alpha}.$$

Lastly, comparing the zeroth-order terms of both transfer functions, an expression of the feedback gain $K^{\text{accel}}_{\dot h h}$ is calculated as:

$$Z_u K^{\text{class}}_h = Z_u K^{\text{accel}}_h,$$
$$\Rightarrow K_{\dot u} K_{\dot u u} K_{u\dot h} K^{\text{class}}_{\dot h h} = K_{\dot u} K_{\dot u \ddot h} K_{\ddot h \dot h} K^{\text{accel}}_{\dot h h},$$
$$\Rightarrow K_{\dot u u} K_{u\dot h} K^{\text{class}}_{\dot h h} = \frac{-1}{Z_u} K_{\dot u u} K_{\ddot h \dot h} K^{\text{accel}}_{\dot h h},$$
$$\Rightarrow K_{u\dot h} K^{\text{class}}_{\dot h h} = \frac{-1}{Z_u} K_{\ddot h \dot h} K^{\text{accel}}_{\dot h h},$$
(53)
$$\Rightarrow \boxed{K^{\text{accel}}_{\dot h h} = \frac{-Z_u K_{u\dot h} K^{\text{class}}_{\dot h h}}{K_{\ddot h \dot h}}}.$$

The block diagrams in figure 18 are used to derive the control laws for both the classical and LAC approaches. In contrast to the classical approach, the LAC approach does not directly command an actuator position, but rather an actuator speed. Therefore,

©2026

both control laws are formulated in terms of the commanded actuator speed $\dot{u}_c$. The control law for the classical approach is given by:

$$\begin{aligned} \dot{u}_c &= (u_c - u)K_{\dot{u}u}, \\ \Rightarrow \dot{u}_c &= \left((\dot{h}_c - \dot{h})K_{u\dot{h}} - u\right) K_{\dot{u}u}, \\ \Rightarrow &\boxed{\dot{u}_c = \left(\left((h_c - h)K^{\text{class}}_{\dot{h}h} - \dot{h}\right) K_{\dot{u}h} - u\right) K_{\dot{u}u}}. \end{aligned} \tag{54}$$

The control law for the LAC approach can be expressed as follows:

$$\begin{aligned} \dot{u}_c &= (\ddot{h}_c - \ddot{h})K_{\dot{u}\ddot{h}}, \\ \Rightarrow \dot{u}_c &= \left((\dot{h}_c - \dot{h})K_{\ddot{h}\dot{h}} - \ddot{h}\right) K_{\dot{u}\ddot{h}}, \\ \Rightarrow &\boxed{\dot{u}_c = \left(\left((h_c - h)K^{\text{accel}}_{\dot{h}h} - \dot{h}\right) K_{\ddot{h}\dot{h}} - \ddot{h}\right) K_{\dot{u}\ddot{h}}}. \end{aligned} \tag{55}$$

Figure 19 presents the system responses of a step altitude command for both the classical and LAC approaches. The identical performance of both approaches observed in the figure validates the feedback gains calculated above.

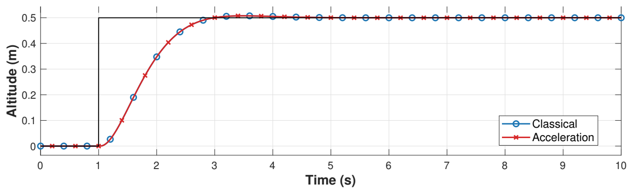

FIG 19. Step response for the classical and LAC approaches